iopscience.iop.org

Home Search Collections Journals About Contact us My IOPscience

A new layer compound Nb_4SiC_3 predicted from first-principles theory

This content has been downloaded from IOPscience. Please scroll down to see the full text.

2009 J. Phys. D: Appl. Phys. 42 075404

(http://iopscience.iop.org/0022-3727/42/7/075404)

View the table of contents for this issue, or go to the journal homepage for more

Download details:

IP Address: 113.108.133.53
This content was downloaded on 18/07/2017 at 06:42

Please note that terms and conditions apply.

You may also be interested in:

First-principles study of electronic structure, mechanical and optical properties of V4AlC3
Chenliang Li, Biao Wang, Yuanshi Li et al.

Elastic, electronic and optical properties of the filled tetrahedral semiconductor LiCdP
A Bouhemadou and R Khenata

Structure of the ternary carbide Ti3SnC2 from ab initio calculations
M B Kanoun and M Jaouen

Pressure-induced effects on elastic and mechanical properties of TiC and TiN: A DFT study
Zhao-Yong Jiao, Shu-Hong Ma, Xian-Zhou Zhang et al.

First principles investigation of protactinium-based oxide-perovskites for flexible opto—electronic devices
Nazia Erum and Muhammad Azhar Iqbal

Phase stability, electronic structure and mechanical properties of molybdenum disilicide: a first-principles investigation
Yingjie Qiao, Hexin Zhang, Changqing Hong et al.

Ab initio investigations of the strontium gallium nitride ternaries Sr3GaN3 and Sr6GaN5: promising materials for optoelectronic
Souraya Goumri-Said, Haci Ozisik, Engin Deligoz et al.

IOP Publishing Journal of Physics D: Applied Physics
J. Phys. D: Appl. Phys. **42** (2009) 075404 (5pp) doi:10.1088/0022-3727/42/7/075404

A new layer compound Nb_4SiC_3 predicted from first-principles theory

Chenliang Li[1], **Jeilai Kuo**[2], **Biao Wang**[3,6], **Yuanshi Li**[4] **and Rui Wang**[5]

[1] School of Astronautics, Harbin Institute of Technology, Harbin, People's Republic of China
[2] School of Physics and Mathematical Sciences, Nanyang Technological University, Singapore
[3] School of Physics and Engineering, Sun Yat-Sen University, Guangzhou, People's Republic of China
[4] Department of Cardiology, The first Clinical College, Harbin Medical University, Harbin, People's Republic of China
[5] Department of Applied Chemistry, Harbin Institute of Technology, Harbin, People's Republic of China

E-mail: lichenliang1980@yahoo.com.cn (B Wang)

Received 24 October 2008, in final form 26 December 2008
Published 12 March 2009

Abstract
We predicted a new layer compound Nb_4SiC_3 using the first-principles method. The structural stability, mechanical, electronic, theoretical hardness and optical properties of Nb_4SiC_3 were investigated. A stable Nb_4SiC_3 phase appears in the α-type crystal structure. Moreover, the predicted Nb_4SiC_3 is a metal and exhibits covalent nature. Nb_4SiC_3 has a theoretical hardness of 10.86 GPa, which is much higher than Nb_4AlC_3; at the same time, it is more ductile than Nb_4AlC_3. The strong covalent bonding in Nb_4SiC_3 is responsible for its high bulk modulus and hardness. Nb_4SiC_3 exhibits slightly anisotropic elasticity. Furthermore, its optical properties are also analysed in detail. It is shown that Nb_4SiC_3 might be a better candidate material as a coating to avoid solar heating than Ti_4AlN_3.

1. Introduction

Layered ternary compounds, $M_{n+1}AX_n$ (where M is an early transition metal, A is an A group element, X is C or N and $n = 1$–3), have received tremendous attention due to their extraordinary mechanical, physical and chemical properties [1]. The layered structure of these compounds results in their unique combination of metallic and ceramic properties, such as high bulk modulus, high melting point, low density, damage tolerance, microscale ductility at room temperature and resistance to thermal shock and high-temperature oxidation [1–4].

Up to now, more than 50 M_2AX compounds, five M_3AX_2 compounds (Ti_3SiC_2, Ti_3GeC_2, Ti_3AlC_2, Ti_3SnC_2 and Ta_3AlC_2) and six M_4AX_3 compounds (Ti_4AlN_3, Ti_4SiC_3, Ti_4GeC_3, Ta_4AlC_3, Nb_4AlC_3 and V_4AlC_3) have been synthesized. Previous studies on M_4AX_3 compounds focused mainly on phase stability, electronic structure, chemical bonding, mechanical and optical properties [5–12]. Recently, Nb_4AlC_3 was synthesized by annealing Nb_2AlC at 1700 °C. Nb_4AlC_3 possessed a low hardness, high fracture toughness and excellent mechanical properties at high temperatures; at the same time, it may display quasi-ductility [13–15]. Although Nb_4AlC_3 has these excellent properties, there may be other compounds with superior properties that remain to be discovered. For example, Nb_4AlC_3 has a low hardness due to the weakness of Nb–Al bonds, and therefore it is likely that the combination of Nb and other atoms will give a new M_4AX_3 compound with a high hardness.

In this paper, we proposed a new layer compound Nb_4SiC_3 and predicted its properties, such as mechanical, electronic and optical properties. We found that Nb_4SiC_3 has better mechanical and optical properties than Nb_4AlC_3 and Ti_4AlN_3.

2. Computational details

The calculations were performed using the CASTEP code based on density functional theory with the generalized gradient approximation (GGA) in the scheme of Perdew–Burke–Ernzerhof [16]. The ion–electron interaction was modelled by ultrasoft Vanderbilt-type pseudopotentials [17]. The elastic constants were calculated by the 'stress–strain' method. Mulliken charges were calculated according to the formalism described by Segall *et al* [18]. A plane-wave cutoff energy of 450 eV was employed throughout

---

[6] Author to whom any correspondence should be addressed.

the calculation. Geometry optimization was achieved using convergence thresholds of 1×10^{-5} eV atom^{-1} for total energy, 0.03 eV Å^{-1} for maximum force and 0.001 Å for displacement. The tolerance in the self-consistent field (SCF) calculation is 1×10^{-6} eV atom^{-1}. For the sampling of the Brillouin zone, the electronic structures and optical properties used $12 \times 12 \times 4$ and $14 \times 14 \times 4$ k-point grids generated according to the Monkhorst–Pack scheme [19], respectively.

The optical properties of Nb_4SiC_3 are investigated by the frequency-dependent dielectric function $\varepsilon(\omega) = \varepsilon_1(\omega) + \iota\varepsilon_2(\omega)$ which is mainly connected with the electronic structures. The imaginary part $\varepsilon_2(\omega)$ of the dielectric function $\varepsilon(\omega)$ is calculated from the momentum matrix elements between the occupied and the unoccupied electronic states and given by

$$\varepsilon_2(\omega) = \frac{2e^2\pi}{\Omega\varepsilon_0}\sum_{k,v,c}|\langle\psi_k^c|\hat{u}\cdot r|\psi_k^v\rangle|^2\delta(E_k^c - E_k^v - E),$$

where ω is the light frequency, e is the electronic charge and ψ_k^c and ψ_k^v are the conduction and valence band wave functions at k, respectively. The real part $\varepsilon_1(\omega)$ is derived from the imaginary part $\varepsilon_2(\omega)$ by the Kramers–Kronig transformation. All other optical constants, such as the absorption spectrum, the energy-loss spectrum and reflectivity, are derived from $\varepsilon_1(\omega)$ and $\varepsilon_2(\omega)$ [20].

3. Results and discussions

3.1. Structural and elastic properties

Nb_4AlC_3 has two types of crystal structures [14]: the α-type has an atom arrangement of ABABACBCBC, while the β-type has an atom arrangement of ABABABABAB. The structural parameters of α- and β-type Nb_4AlC_3 are presented in table 1. The structures of α- and β-type Nb_4SiC_3 were constructed by substituting the Al atoms with the Si atoms in the two types of crystal structures of Nb_4AlC_3, respectively. The predicted lattice parameters and atom positions of the different Nb_4SiC_3 phases are also displayed in table 1. Density functional theory with GGA usually overestimates the lattice parameters and underestimates the bulk moduli [21]. We also calculated the total energies of the different Nb_4SiC_3 phases. The total energy (−13 567.32 eV) of α-Nb_4SiC_3 is lower than that (−13 566.41 eV) of β-Nb_4SiC_3. Therefore, a stable Nb_4SiC_3 phase appears in the α-type crystal structure, which is the same as Nb_4AlC_3. In the following investigation, we focus mainly on the properties of α-Nb_4SiC_3.

In order to study the mechanical properties of α-Nb_4SiC_3, we calculated its elastic constants, bulk modulus B, shear modulus G and Young's moduli E. The results are shown in table 1, together with the theoretical results of α-Nb_4AlC_3 for comparison. The C_{11} of α-Nb_4SiC_3 is 11 GPa smaller than that of α-Nb_4AlC_3, and this leads to the lower resistances against the principal strain ε_{11}. However, the C_{33} of α-Nb_4SiC_3 is 46 GPa larger than that of α-Nb_4AlC_3, and this leads to higher resistances against the principal strain ε_{33}. The C_{44} of α-Nb_4SiC_3 is 34 GPa larger than that of α-Nb_4AlC_3, thereby higher resistances to basal and prismatic shear deformations. The bulk modulus B of α-Nb_4SiC_3 is higher than that of α-Nb_4AlC_3, and this leads to a higher resistance to the volume change. The shear modulus G of α-Nb_4SiC_3 is very close to that of α-Nb_4AlC_3. Therefore, α-Nb_4SiC_3 has the same resistance to the shape change as α-Nb_4AlC_3. In order to evaluate the elastic anisotropy of the material, we also calculated the ratio between linear compressibility coefficients k_c/k_a. For hexagonal crystals, k_c/k_a can be expressed as $k_c/k_a = (C_{11} + C_{12} - 2C_{13})/(C_{33} - C_{13})$. The k_c/k_a value of α-Nb_4SiC_3 is equal to 1.15, and therefore it has a slight anisotropy on elasticity.

On the other hand, the elastic constants of α-Nb_4SiC_3 can satisfy the well-known Born stability criteria [22]:

$$C_{11} > 0, \qquad C_{11} - C_{12} > 0, \qquad C_{44} > 0,$$

$$(C_{11} + C_{12})C_{33} - 2C_{13}^2 > 0.$$

It is known that α-Nb_4SiC_3 is mechanically stable under elastic strain perturbations. The ductility of a material can be roughly estimated by the value of shear-modulus-to-bulk-modulus ratios (G/B) [23–27]. A low (high) G/B value

Table 1. Predicted lattice parameters (Å), atomic positions, elastic constants C_{ij} (GPa), bulk modulus B (GPa), shear modulus G (GPa), Young's moduli E (GPa) and shear-modulus-to-bulk-modulus ratio (G/B) of Nb_4SiC_3.

	α-Nb_4SiC_3	β-Nb_4SiC_3	α-$Nb_4AlC_3^a$	β-$Nb_4AlC_3^a$
Space group	$P6_3/mmc$	$P6_3/mmc$	$P6_3/mmc$	$P6_3/mmc$
Lattice constants	$a = 3.1819$	$a = 3.1326$	$a = 3.1296$	$a = 3.1128$
	$c = 22.9877$	$c = 23.6468$	$c = 24.1208$	$c = 24.7089$
Atomic position				
Nb1	(1/3, 2/3, 0.0574)	(1/3, 2/3, 0.05655)	(1/3, 2/3, 0.0553)	(1/3, 2/3, 0.05449)
Nb2	(0, 0, 0.16408)	(1/3, 2/3, 0.6646)	(0, 0, 0.1574)	(1/3, 2/3, 0.6581)
Si/Al	(1/3, 2/3, 1/4)	(1/3, 2/3, 1/4)	(1/3, 2/3, 1/4)	(1/3, 2/3, 1/4)
C1	(0, 0, 0)	(0, 0, 0)	(0, 0, 0)	(0, 0, 0)
C2	(2/3,1/3, 0.113 07)	(0, 0, 0.113 97)	(2/3, 1/3, 0.1086)	(0, 0, 0.109 99)
C_{11}, C_{33}, C_{44}	403, 374, 195		413, 328, 161	
C_{12}, C_{13}	167, 165		124, 135	
G	142		144	
B	241		214	
E	$E_x = 303$, $E_z = 278$		$E_x = 344$, $E_z = 260$	
G/B	0.59		0.67	

[a] Reference [14].

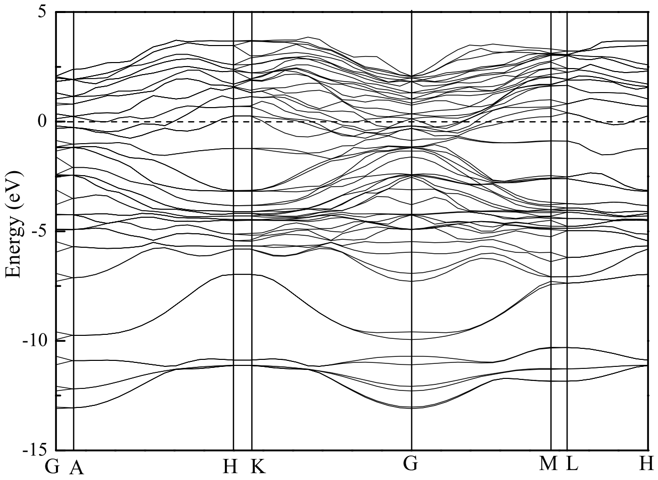

Figure 1. Energy band structure of α-Nb_4SiC_3.

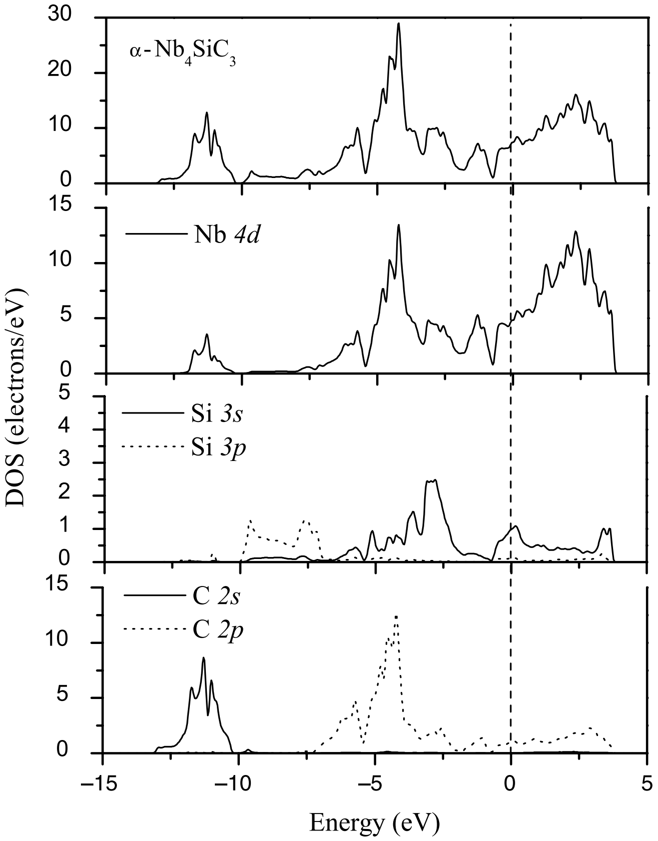

Figure 2. Total and partial DOS of α-Nb_4SiC_3.

shows ductility (brittleness). The G/B value of α-Nb_4SiC_3 is lower than that of α-Nb_4AlC_3. Therefore, α-Nb_4SiC_3 is more ductile than α-Nb_4AlC_3 and exhibits a high shear deformation resistance.

3.2. Electronic properties and theoretical hardness

The energy band structure and densities of states (DOSs) of α-Nb_4SiC_3 are shown in figures 1 and 2, respectively. The energy band structure is calculated along the high-symmetry directions in the Brillouin zone. There are many bands crossing the Fermi level, suggesting that Nb_4SiC_3 is a metal. The lowest energy bands from −13 to −10 eV are dominated by the hybridized Nb 4d and C 2s states. The energy bands between −10 and −7.5 eV consist mainly of Si 3p states, with little contribution from its 3*s* states. The energy bands between −7.5 and −0.76 eV are dominated by the hybridized Nb 4d/Si 3s and C 2p states. Therefore, Nb_4SiC_3 appears to have covalent nature. Moreover, the peaks of Si 3s are weaker than those of the Nb 4d and C 2p states. The number of peaks was also less than those of Nb and C. Furthermore, the hybridized Nb 4d and C 2s states appear in a lower energy range. These results indicate that the Nb–C bond is stronger than the Nb–Si bond. In addition, the energy bands near and above the Fermi level are attributed to Nb 4d states and antibonding states.

Table 2. Calculated Mulliken bond overlap population P^{μ}, bond length d^{μ} (Å) and Vickers hardness $H_{v\text{calc}}$ (GPa) of α-Nb_4SiC_3.

Bond	d^{μ}	P^{μ}	$P^{\mu'}$	ν_b^{μ}	H_v^{μ}	$H_{v\text{calc}}$
C–Nb	2.179	0.99	0.021	9.882	15.76	10.86
	2.239	1.00	0.021	10.72	13.9	
	2.262	1.00	0.021	11.054	13.21	
Si–Nb	2.697	0.88	0.021	18.736	4.81	

We also performed the Mulliken bond populations in order to understand the bonding behaviour of Nb_4SiC_3 and obtain its theoretical Vickers hardness. The theoretical hardness of crystals with metallic bonding can be calculated as follows [28, 29]:

$$H_v = \left[\prod^{\mu}(H_v^{\mu})^{n^{\mu}}\right]^{1/\sum n^{\mu}}$$

$$H_v^{\mu}\ (\text{GPa}) = 740(P^{\mu} - P^{\mu'})(\nu_b^{\mu})^{-5/3},$$

where P^{μ} is the Mulliken population of the μ-type bond, $P^{\mu'}$ is the metallic population of the μ-type bond and ν_b^{μ} is the volume of a bond of type μ. The calculated results are shown in table 2. The bond populations indicate the overlap degree of the electron cloud of two bonding atoms. Its highest and lowest values imply that the chemical bond exhibits strong covalency and ionicity, respectively. It can be seen that the C–Nb bonds possessed stronger covalent bonding than the Si–Nb bonds. The results are consistent with our DOS calculation. Moreover, the hardness of Nb_4SiC_3 (10.86 GPa) is higher than Nb_4AlC_3 (2.6 GPa) [15]. The strong covalent bonding in Nb_4SiC_3 is responsible for its high bulk modulus and hardness.

3.3. Optical properties

The calculated results on the dielectric function, the absorption spectrum, conductivity and the energy-loss spectrum are shown in figures 3(*a*)–(*d*), respectively. In our calculation, we used a 0.5 eV Gaussian smearing. The imaginary part $\varepsilon_2(\omega)$ of the dielectric function is very large below 3 eV, which is due to transitions within the Nb 4d bands, and the $\varepsilon_2(\omega)$ spectrum above 3 eV arises from Si/C p → Nb d electronic transitions. The large negative value of $\varepsilon_1(\omega)$ indicates that the Nb_4SiC_3 crystal has a Drude-like behaviour. The absorption spectrum rises sharply below 8.38 eV and presents three peaks between

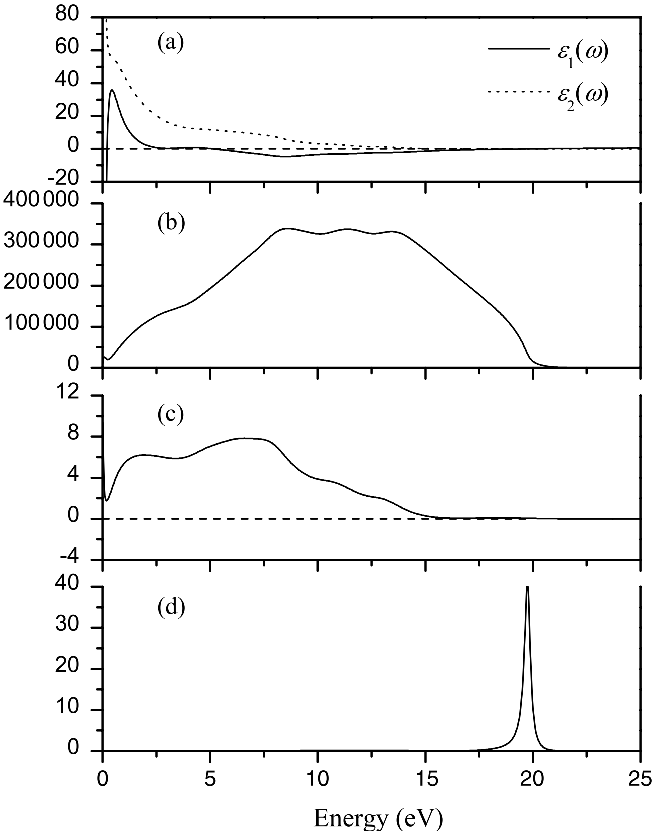

Figure 3. Optical constants ofα-Nb_4SiC_3. (*a*) Imaginary part $\varepsilon_2(\omega)$ and real part $\varepsilon_1(\omega)$ of the dielectric function $\varepsilon(\omega)$, (*b*) absorption spectrum, (*c*) photoconductivity and (*d*) energy-loss spectrum.

9 and 14 eV, and then decreases rapidly in the high-energy region. Three peaks are associated with the transition from Si/C p to Nb d states. Photoconductivity is the increase in the electrical conductivity of a material as a result of absorbing photons [30]. For Nb_4SiC_3, there is photoconductivity when the photon energy is equal to 0 eV. The reason is that Nb_4SiC_3 has no band gap. Therefore, photocurrent can be generated within a wide range of photon energies. The energy-loss spectrum describes the energy loss of a fast electron traversing in the material [31]. Its peak is defined as the bulk plasma frequency ω_ρ, which occurs where $\varepsilon_2 < 1$ and ε_1 reaches the zero point [32, 33].

The reflectivity spectra of Nb_4SiC_3, Ti_4AlN_3 [12] and TiN [34] are compared in figure 4. The spectrum of TiN shows a sharp dip from 1.5 to 2.7 eV. Moreover, TiN has a goldlike colour due to high reflectivity for red light and low reflectivity for blue light [35]. Therefore, the reflectance spectrum of TiN is selective. Compared with the reflectance spectrum of TiN, that of Nb_4SiC_3 has no strong edge and colour and does not greatly change at different wavelengths. Therefore, the reflectance spectrum of Nb_4SiC_3 is nonselective and very similar to that of Ti_4AlN_3. According to the nonselective characteristic of the reflectance spectrum of Ti_4AlN_3, Li *et al* [12] concluded that Ti_4AlN_3 could reduce solar heating and enhance the infrared emittance, and therefore the equilibrium temperature of its surface will be moderate in strong sunlight. Based on the conclusion, Nb_4SiC_3 might also be used as a coating to avoid solar heating. Moreover, Nb_4SiC_3 may well be a better material to avoid solar heating because the reflectance spectrum of Nb_4SiC_3 exhibits less change at different wavelengths than that of Ti_4AlN_3. On the other hand, we also find that the reflectivity of Nb_4SiC_3 is always higher than that of Ti_4AlN_3. Therefore, the capability of Nb_4SiC_3 to reflect solar light is stronger than Ti_4AlN_3.

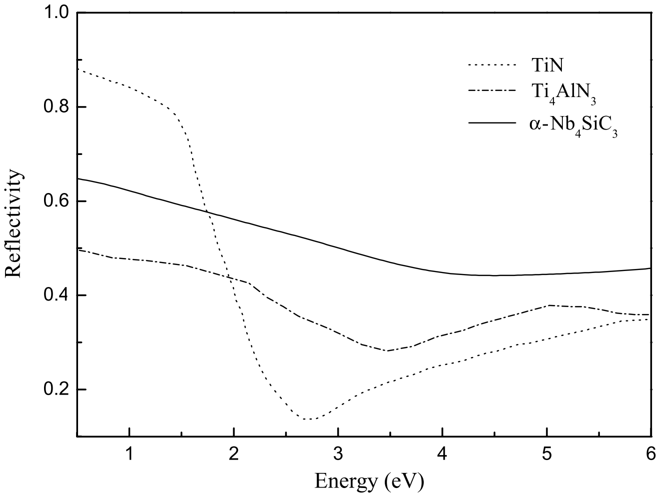

Figure 4. Reflectivity spectra of α-Nb_4SiC_3, Ti_4AlN_3 [12] and TiN [34].

4. Conclusions

In summary, a new layer compound Nb_4SiC_3 has been predicted using the first-principles method. We investigated its structural stability, mechanical properties, electronic structure, theoretical hardness and optical properties. A stable Nb_4SiC_3 phase appears in the α-type crystal structure. The electronic structures of Nb_4SiC_3 reveal that it is a metal and exhibits covalent nature. Moreover, the C–Nb bonds possessed stronger covalent bonding than the Si–Nb bonds. The strong covalent bonding in Nb_4SiC_3 is responsible for its high bulk modulus and hardness. The elastic constants, bulk modulus, shear modulus and Young's moduli of α-Nb_4SiC_3 are calculated. The results show that Nb_4SiC_3 is more ductile and has a higher hardness than α-Nb_4AlC_3. α-Nb_4SiC_3 also exhibits slight anisotropic elasticity. Finally, the dielectric function, the absorption spectrum, the conductivity, the energy-loss spectrum and reflectivity were obtained and discussed in detail. It is shown that Nb_4SiC_3 might be a better candidate material as a coating to avoid solar heating than Ti_4AlN_3. We hope that the theoretical predictions will inspire experimental investigation on Nb_4SiC_3.

Acknowledgments

This project was supported by the National Natural Science Foundation of China (10572155 and 10172030) and the Ministry of Education PRC Special Scientific Research Fund for Doctor Subjects in Colleges and Universities (20060558070).

References

[1] Barsoum M W 2000 *Prog. Solid. State. Chem.* **28** 201

[2] Grechnev A, Li S, Ahuja R, Eriksson O, Jansson U and Wilhelmsson O 2004 *Appl. Phys. Lett.* **85** 3071

[3] Barsoum M W and El-Raghy T 1996 *J. Am. Ceram. Soc.* **79** 1953

[4] Manoun B, Saxena S K, EI-Raghy T and Barsoum M W 2006 *Appl. Phys. Lett.* **88** 201902

[5] Magnuson M, Mattesini M, Wilhelmsson O, Emmerlich J, Palmquist J-P, Li S, Ahuja R, Hultman L, Eriksson O and Jansson U 2006 *Phys. Rev.* B **74** 205102

[6] Sun Z M and Zhou Y C 2002 *J. Phys. Soc. Japan* **71** 1313

[7] Holm B, Ahuja R, Li S and Johansson B 2002 *J. Appl. Phys.* **91** 9874

[8] Lin Z J, Zhou M J, Zhou Y C, Li M S and Wang J Y 2006 *J. Mater. Res.* **21** 2587

[9] Eklund P, Palmquist J-P, Howing J, Trinh D H, El-Raghy T, Hogberg H and Hultman L 2007 *Acta Mater.* **55** 4723

[10] Du Y L, Sun Z M, Hashimoto H and Tian W B 2008 *Solid State Commun.* **147** 246

[11] Du Y L, Sun Z M, Hashimoto H and Tian W B 2008 *Solid State Commun.* **145** 461

[12] Li S, Ahuja R, Barsoum M W, Jena P and Johansson B 2008 *Appl. Phys. Lett.* **92** 221907

[13] Hu C F, Li F Z, Zhang J, Wang J M, Wang J Y and Zhou Y C 2007 *Scr. Mater.* **57** 893

[14] Wang J M, Wang J Y, Zhou Y C and Hu C F 2008 *Acta Mater.* **56** 1511

[15] Hu C F, Li F Z, He L F, Liu M Y, Zhang J, Wang J M, Bao Y W, Wang J Y and Zhou Y C 2008 *J. Am. Ceram. Soc.* **91** 2258

[16] Perdew J P, Burke K and Ernzerhof M 1996 *Phys. Rev. Lett.* **77** 3865

[17] Vanderbilt D 1990 *Phys. Rev.* B **41** 7892

[18] Segall M D, Pickard C J, Shah R and Payne M C 1996 *Mol. Phys.* **89** 571

[19] Monkhorst H J and Pack J D 1976 *Phys. Rev.* B **13** 5188

[20] Saha S, Sinha T P and Mookerjee A 1976 *Phys. Rev.* B **13** 5188

[21] Dal Corso A, Pasquarello A, Baldereschi A and Car R 1996 *Phys. Rev.* B **53** 1180

[22] Hu Q K, Wu Q H, Ma Y M, Zhang L J, Liu Z Y, He J L, Sun H, Wang H T and Tian Y J 2006 *Phys. Rev.* B **73** 214116

[23] Wang J Y, Zhou Y C and Lin Z J 2005 *Appl. Phys. Lett.* **87** 051902

[24] Vitos L, Korzhavyi P A and Johansson B 2003 *Nature Mater.* **2** 25

[25] Music D, Sun Z M and Schneider J M 2005 *Phys. Rev.* B **71** 092102

[26] Music D and Schneider J M 2006 *Appl. Phys. Lett.* **88** 031914

[27] Wang N, Yu W Y, Tang B Y, Peng L M and Ding W J 2008 *J. Phys. D: Appl. Phys.* **41** 195408

[28] Gao F M 2006 *Phys. Rev.* B **73** 132104

[29] Gou H Y, Hou L, Zhang J W and Gao F M 2008 *Appl. Phys. Lett.* **92** 241901

[30] Sun J, Zhou X F, Fan Y X, Chen J and Wang H T 2006 *Phys. Rev.* B **73** 045108

[31] Xu M, Wang S Y, Yin G, Li J, Zheng Y X and Chen L Y 2006 *Appl. Phys. Lett.* **89** 151908

[32] Saniz R, Ye L H, Shishidou T and Freeman A J 2006 *Phys. Rev.* B **74** 014209

[33] Almeida de J S and Ahuja R 2006 *Phys. Rev.* B **73** 165102

[34] Karlsson B 1981 Optical properties of solids for solar energy conversion *PhD Thesis* Acta Universitatis Upsaliensis, Uppsala, Sweden

[35] Delin A, Eriksson O, Ahuja R, Johansson B, Brooks M S S, Gasche T, Auluck S and Wills J M 1996 *Phys. Rev.* B **54** 1673